REPORT DOCUMENTATION PAGE

Form Approved
OMB No. 0704-0188

PLEASE DO NOT RETURN YOUR FORM TO THE ABOVE ORGANIZATION.

1. REPORT DATE *(DD-MM-YYYY)*	2. REPORT TYPE	3. DATES COVERED *(From - To)*
30-05-2011	Final	01-12-2008 to 30-03-2011

4. TITLE AND SUBTITLE
Algorithm Development for the Multi-Fluid Plasma Model

5a. CONTRACT NUMBER
FA9550-09-1-0135

5b. GRANT NUMBER
FA9550-09-1-0135

5c. PROGRAM ELEMENT NUMBER

6. AUTHOR(S)
Uri Shumlak

5d. PROJECT NUMBER

5e. TASK NUMBER

5f. WORK UNIT NUMBER

7. PERFORMING ORGANIZATION NAME(S) AND ADDRESS(ES)
University of Washington
Aerospace & Energetics Research Program
Box 352250
Seattle, WA 98195-2250

8. PERFORMING ORGANIZATION REPORT NUMBER

9. SPONSORING/MONITORING AGENCY NAME(S) AND ADDRESS(ES)
Dr. Fariba Fahroo
Program Manager, Computational Mathematics
AFOSR/NL
875 N. Randolph St, Rm 3112
Arlington, VA 22203

10. SPONSOR/MONITOR'S ACRONYM(S)
AFOSR/NL

11. SPONSOR/MONITOR'S REPORT NUMBER(S)
AFRL-OSR-VA-TR-2012-0925

12. DISTRIBUTION/AVAILABILITY STATEMENT
Approved for public release

13. SUPPLEMENTARY NOTES

14. ABSTRACT
An algorithm is developed based on the multi-fluid plasma model derived from moments of the Boltzmann equation. Large mass differences between electrons and ions introduce disparate temporal and spatial scales and require a numerical algorithm with sufficient accuracy to capture the multiple scales. The multi-fluid capability is not limited to two species. Plasma with multiple components can be modeled, e.g. impurity ions, neutral gas. The multi-fluid equations are derived in divergence form for the naturally occurring conserved variables. The source terms of the multi-fluid plasma model couple the fluids to themselves (interspecies interactions) and to the electromagnetic fields. The solution and evolution must be tightly coupled to prevent unstable numerical oscillations. A discontinuous Galerkin method is developed to solve the governing equations on a computational grid and to simulate plasma phenomena. Interspecies interactions also occur through collisional source terms that account for the direct transfer of momentum and energy. In addition to the plasma and electrodynamic physics, the multi-fluid plasma model captures atomic physics in the form reaction rate equations for ionization and recombination, which introduce new temporal scales to the plasma dynamics model.

15. SUBJECT TERMS
advanced plasma models, high-order algorithms, multiscale physics, mathematically stiff equations

16. SECURITY CLASSIFICATION OF:			17. LIMITATION OF ABSTRACT	18. NUMBER OF PAGES	19a. NAME OF RESPONSIBLE PERSON
a. REPORT	b. ABSTRACT	c. THIS PAGE			Uri Shumlak
U	U	U	UU	23	19b. TELEPHONE NUMBER *(Include area code)* 206-616-1986

Final Performance Report (12/1/08 – 3/30/11)

AFOSR Grant No. FA9550-09-1-0135

"ALGORITHM DEVELOPMENT FOR THE MULTI-FLUID PLASMA MODEL"

Submitted to

Dr. Fariba Fahroo
Program Manager, Computational Mathematics
Air Force Office of Scientific Research / NL
875 N. Randolph St, Rm 3112
Arlington, VA 22203

University of Washington
Department of Aeronautics and Astronautics
Aerospace & Energetics Research Program
Box 352250
Seattle, WA 98195-2250

Dr. Uri Shumlak
Principal Investigator

5/30/11

ALGORITHM DEVELOPMENT FOR THE MULTI-FLUID PLASMA MODEL

AFOSR Grant No. FA9550-09-1-0135

U. Shumlak

Department of Aeronautics and Astronautics
Aerospace & Energetics Research Program
University of Washington

Abstract

An algorithm is developed based on the multi-fluid plasma model derived from moments of the Boltzmann equation. The MHD (magnetohydrodynamic) model involves assumptions that limit its applicability. The multi-fluid plasma model only assumes local thermodynamic equilibrium and, therefore, accurately models the appropriate physical processes. The multi-fluid plasma model typically has two fluids representing electron and ion species. Large mass differences between electrons and ions introduce disparate temporal and spatial scales and require a numerical algorithm with sufficient accuracy to capture the multiple scales. The multi-fluid capability is not limited to two species. Plasma with multiple components can be modeled, e.g. impurity ions, neutral gas. The multi-fluid equations are derived in divergence form for the naturally occurring conserved variables. The source terms of the multi-fluid plasma model couple the fluids to themselves (interspecies interactions) and to the electromagnetic fields. The solution and evolution must be tightly coupled to prevent unstable numerical oscillations. The electromagnetic field equations are solved by applying correction potentials or by using a mixed potential formulation to eliminate any components of the fields that violate the divergence constraints. A discontinuous Galerkin method is developed to solve the governing equations on a computational grid and to simulate plasma phenomena. Interspecies interactions also occur through collisional source terms that account for the direct transfer of momentum and energy. In addition to the plasma and electrodynamic physics, the multi-fluid plasma model captures atomic physics in the form reaction rate equations for ionization and recombination, which introduce new temporal scales to the plasma dynamics model. The numerical algorithm must treat the inherent stiffness introduced by the multiple physical effects of the model. Fully implicit and semi-implicit treatments have been implemented with the semi-implicit treatment showing promise for a more optimum method. Nonreflecting boundary conditions using a lacunae-based method have been implemented and provide higher solution fidelity for open boundary problems.

1 Executive Summary

This project represents a two-year effort to develop a new algorithm for plasma simulations based on the multi-fluid plasma model. The algorithm is capable of three-dimensional, time-dependent plasma simulations that capture the multi-physics and multi-scale effects of the complete multi-fluid plasma model. The multi-fluid plasma equations is formulated in divergence form which includes source terms. The source terms couple the fluids to the electromagnetic fields, account for collisions between the fluids, and provide sinks and sources from the atomic reactions. A high-order algorithm is developed that solves the complete multi-fluid plasma model such that equilibrium, perturbation, and transient phenomena can be accurately simulated. The algorithm uses the discontinuous Galerkin method to achieve high-order accuracy. Novel numerical approaches for time integration are investigated to perform simulations that are not limited by the shortest timescale of the system. These methods include fully implicit backward difference and a semi-implicit treatment. The algorithm takes advantage of the parallel computing architectures that are available locally and at the Major Shared Resource Centers (parallel workstation cluster, Dell PowerEdge, Cray XD1, and others). The new algorithm has been benchmarked against known analytical results, previously published results, and experimental data from the Air Force Research Laboratories [the field reversed configuration (FRC) implosions for magnetized target fusion (MTF) at Kirtland AFB and FRC experiments at the University of Washington].

Many plasma simulation codes are currently based on the MHD (magnetohydrodynamic) model. The derivation of the MHD model involves several assumptions that severely limit its applicability. MHD simulations of several technologies important to the USAF have failed to predict the experimentally observed plasma behavior, e.g. stability of field reversed configurations. Recent success with the two-fluid plasma model has provided a development path for plasma simulations that are more physically accurate and capable than MHD models. [1–6] Building on the successful development of the two-fluid model, a plasma simulation algorithm is developed for the multi-fluid plasma model. The multi-fluid plasma model only assumes local thermodynamic equilibrium within each fluid and is, therefore, more physically accurate and capable than MHD models. The separate electron and ion response is accurately represented, as well as, multi-component plasmas that can include impurities, neutrals.

The multi-fluid model is formulated in conservation form and lends itself naturally to accurate fluid models. For example, an approximate Riemann solver is developed for the two-fluid plasma model to compute the fluxes in a stable and accurate manner. Several methods are investigated to solve the electromagnetic field model, which includes the source terms and divergence constraints. These methods include a purely hyperbolic formulation of the Maxwell's equation and a mixed potential formulation. The plasma fluids (electrons and ions) and the electromagnetic fields communicate through the source terms. The fluid momentum and energy equations have source terms that

depend on $\mathbf{E}$ and $\mathbf{B}$. The electromagnetic equations have source terms that depend on $\mathbf{v}_i$ and $\mathbf{v}_e$ (Ampere's law) and n_i and n_e (Gauss's equation). All fluids (plasma and neutral) communicate through scattering collisions and atomic reactions that appear as source terms. Accurately coupling the source terms is important both for numerical stability and for modeling plasmas where large equilibrium forces exist.

The multi-fluid algorithm uses a discontinuous Galerkin, finite element method for the spatial representation and a TVD Runge-Kutta method for the time advance. [2] Solutions are found with up to 16^{th} order spatial accuracy and 3^{rd} order temporal accuracy. [7] The multi-fluid plasma algorithm is used to model multiscale physics of current-carrying plasmas, such as the Z-pinch [4] and the field reversed configuration (FRC) [5]. These plasma configurations balance large equilibrium forces between the plasma pressure and the electromagnetic pressure. The high-order algorithm is seen to significantly improve the ability to maintain equilibrium with no artificial decay. [7]

Domain truncation is accomplished by implementing open boundary conditions that are based on lacunae methods. The open domain boundary is appended with an exterior domain that matches the interior solution and then damps the solution before artificial reflections develop. Multi-fluid and arbitrarily complex geometry capability has been demonstrated. [8] Plasma formation process is modeled in a two-dimensional geometry which produces a plasma from the collisions of electrons and neutrals. During the initial formation a Langmuir wave is observed to propagate. FRC simulations are performed in a five-block cylindrical grid. The simulation results show the development of short wavelength drift turbulence.

The divergence constraints of Maxwell's equations can be difficult to satisfy with the presence of current and charge sources on an arbitrary computational grid. The divergence constraints are satisfied by reformulating Maxwell's equations to include correction potentials. The approach involves coupling the divergence constraint equations with the time-dependent field equations to form a purely hyperbolic equation set. [9] An alternative formulation of Maxwell's equations using mixed potential is also implemented. The mixed potential formulation automatically satisfies the divergence constraints; however, a gauge condition must then be enforced.

This project was performed by Prof. Uri Shumlak and graduate students Robert Lilly, Noah Reddell, Eder Sousa, Bhuvana Srinivasan, and Andree Susanto. This project resulted in doctoral dissertations and master thesis:

- Bhuvana Srinivasan, "Numerical Methods for 3-dimensional Magnetic Confinement Configurations using Two-Fluid Plasma Equations", Ph.D. 2010.
- Andree Susanto, "Development of Electromagnetic Solvers for Use with The Two-Fluid Plasma Algorithm", M.S. 2009.

These dissertations and theses can be obtained from the University of Washington library system or from the project website, http://www.aa.washington.edu/research/cfdlab/.

Archival journal and conference papers were published reporting on the work from this project:

- U. Shumlak, R. Lilly, N. Reddell, E. Sousa, and B. Srinivasan, "Advanced physics calculations using a multi-fluid plasma model", *Computer Physics Communications* **182** 1767-1770 (2011).
- B. Srinivasan, A. Hakim, and U. Shumlak, "Numerical methods for two-fluid dispersive fast MHD phenomena", *Communications in Computational Physics* **10** (3), 183-215 (2011).
- J. Loverich, A. Hakim, and U. Shumlak, "A discontinuous Galerkin method for ideal two-fluid plasma equations", *Communications in Computational Physics* **9**, 240-268 (2011).
- A. Hakim and U. Shumlak, "Two-fluid physics and field-reversed configurations", *Physics of Plasmas* **14**, 055911 (2007).

2 Project Results

Plasmas are essential to many technologies that are important to the Air Force, some of which have dual-use potential. These applications include portable pulsed power systems, high power microwave devices, drag reduction for hypersonic vehicles, advanced plasma thrusters for space propulsion, nuclear weapons effects simulations, radiation production for counter proliferation, and fusion for power generation. In general, plasmas fall into a density regime where they exhibit both collective (fluid) behavior and individual (particle) behavior. The intermediate regime complicates the computational modeling of plasmas.

2.1 Plasma Models — Kinetic, PIC, MHD, Multi-Fluid

Plasmas may be most accurately modeled using kinetic theory. The plasma is described by distribution functions in physical space, velocity space, and time, $f(\mathbf{x}, \mathbf{v}, t)$. The evolution of the plasma is then modeled by the Boltzmann equation.

$$\frac{\partial f_\alpha}{\partial t} + \mathbf{v}_\alpha \cdot \frac{\partial f_\alpha}{\partial \mathbf{x}} + \frac{q_\alpha}{m_\alpha} \left(\mathbf{E} + \mathbf{v}_\alpha \times \mathbf{B} \right) \cdot \frac{\partial f_\alpha}{\partial \mathbf{v}} = \left. \frac{\partial f_\alpha}{\partial t} \right|_{collisions} \tag{1}$$

for each plasma species α = ions, electrons. The Boltzmann equation coupled with Maxwell's equations for electromagnetic fields completely describe the plasma dynamics. [10–12] However, the Boltzmann equation is seven dimensional. As a consequence of the large dimensionality plasma simulations using the Boltzmann equation are only used in very limited applications with narrow distributions, small spatial extent, and short time durations. [13, 14] The seven dimensional space is further exacerbated by the high velocity space

that is unused except for tail of the distribution or energetic beams. Boundary conditions are difficult to implement in kinetic simulations.

Particle in cell (PIC) plasma model apply the Boltzmann equation to representative superparticles which are far fewer (10^7) than the number of particles in the actual plasma (10^{20}). [15] PIC simulations have similar limitations as simulations using kinetic theory due to statistical errors caused by the fewer superparticles. Boundary conditions are also difficult to implement in PIC simulations.

The other end of the spectrum in plasma model involves taking moments of the Boltzmann equation and averaging over velocity space for each species which implicitly assumes local thermodynamic equilibrium. The resulting equations comprise the multi-fluid plasma model, where a fluid is defined for each species, e.g. electrons, ions, neutrals. When only two fluids, electrons and ions, are included, the resulting system is the two-fluid plasma model. [1] The two-fluid equations can be combined to form the MHD model. [16] However, in the process several approximations are made which limit the applicability of the MHD model to low frequency and ignores the electron mass and finite Larmor radius effects.

The MHD model treats the plasma like a conducting fluid and assigning macroscopic parameters to describe its particle-like interactions. Plasma simulation algorithms based on the MHD model have been very successful in modeling plasma dynamics and other phenomena. Codes such as MACH2 are based on arbitrary Lagrangian/Eulerian formulations. [17] ALE codes are well suited for simulating plasma phenomena involving moving interfaces. [18] However, ALE codes cannot be formulated as conservation laws and lack many of the inherent conservative properties. The MHD model has been successfully implemented in conservative form to simulate realistic three-dimensional geometries. [19, 20]

A severe limitation of the MHD model is the treatment the Hall effect and diamagnetic terms. These terms represent the separate motions of the ions and electrons. The Hall effect and diamagnetic terms also account for ion current and the finite ion Larmor radius. These effects are important in many applications such as electric space propulsion thrusters: Hall thrusters, magnetoplasmadynamic (MPD) thrusters, Lorentz force thrusters. The Hall term is also believed to be important to electrode effects such as anode and cathode fall which greatly affect many directly coupled plasma applications. Furthermore, the Hall and diamagnetic effects may be important for hypersonic flow applications. [21]

The Hall terms can be difficult to stabilize because they lead to the whistler wave branch of the dispersion relation. The phase and group velocities of the whistler wave increase with frequency. The velocities become large even for modest values of the Hall parameter. See Fig. 1 for the dispersion diagram.

A semi-implicit technique has been applied to treat the Hall term in a Hall-MHD model. [22, 23] After the hyperbolic terms of the MHD equations are advanced, the Hall terms are treated independently. The conserved variables

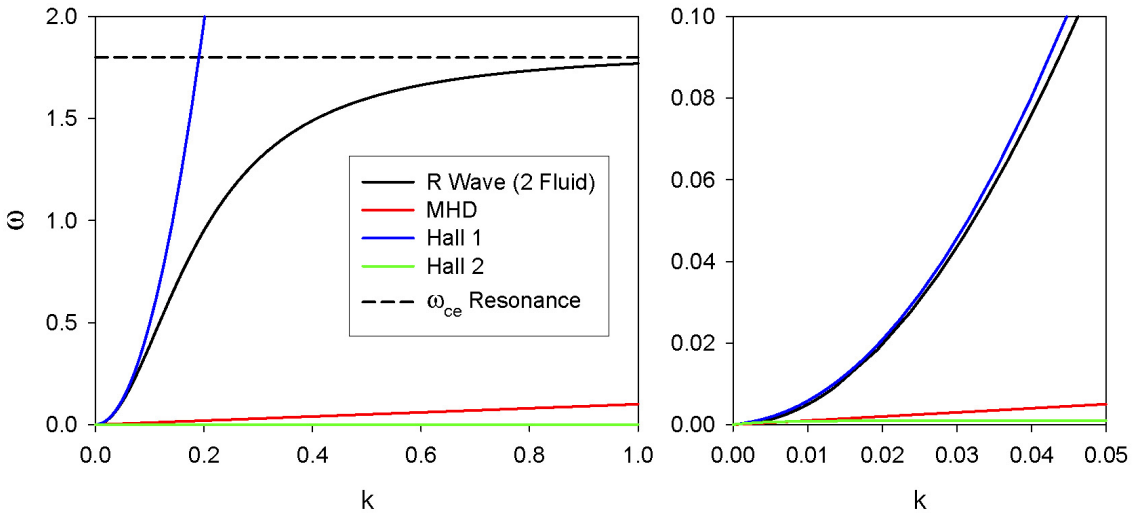

Figure 1: Dispersion relations for the two-fluid plasma model and for the Hall-MHD plasma model that results when asymptotic approximations are applied to the two-fluid plasma model. For small wave numbers and low frequencies (right plot), the upper branch of the Hall-MHD wave follows the R wave of the two-fluid model. However, the waves diverge and the Hall-MHD wave fails to follow the resonance at the cyclotron frequency. The wave speed grows without bound. Artificial hyper-resistivity is required to damp this branch of the Hall-MHD wave.

are then corrected. The procedure can be computationally intensive. The operator stencil uses 5 points in the sweep direction and 3 points in each orthogonal direction. The complete operator stencil is 45 points. The semi-implicit method works adequately for small Hall parameters, but becomes unstable or slow to converge for the large Hall parameters often seen in applications.

As mentioned above, the multi-fluid plasma model is more complete than either the MHD or Hall-MHD model. The multi-fluid plasma model resolves plasma oscillations and speed of light propagation. However, many applications are adequately modeled by lower frequency dynamics. Asymptotic approximations ($m_e \to 0$, $c \to \infty$) have been applied to the two-fluid plasma model to eliminate the high frequency waves that limit the maximum numerical time step. Neglecting electron inertia removes the limitation due to the electron plasma and cyclotron frequencies. Infinite light speed removes the limitation due to light transit times. The asymptotic approximations reduce the two-fluid plasma model to the Hall-MHD model. However, applying these approximations fundamentally changes the dispersion relation, as evident in Fig. 1, and introduces unphysical wave behavior. Specifically, the phase and group velocities of a Hall-MHD wave increase without bound with wave number. The large wave speeds increases the stiffness of the equation system making accurate numerical solutions difficult. Furthermore, the maximum wave number is usually set by either the computational mesh spacing ($k_{max} \propto \Delta x$) or by an artificial resistivity. Rigorous convergence studies are difficult with the simpler plasma models since decreasing Δx leads to larger k_{max} and shorter wavelength phenomena.

2.2 Multi-Fluid Plasma Algorithm

The complexity of the multi-fluid model is greater the MHD model but significantly less than the kinetic model. In this project a new algorithm is developed that solves the multi-fluid plasma model using an approximate Riemann solver. [1] The method tracks the wave propagation across the domain based on conservation laws.

The governing equations for the multi-fluid plasma model (including the electromagnetic equations) are expressed in divergence form. Similar to the two-fluid plasma model, the governing equations for the multi-fluid plasma models are derived by taking moments of the Boltzmann equation, Eq. (1), for each species. Local thermodynamic equilibrium within each fluid is assumed. The fluid variables are derived by taking moments of the distribution function.

The evolution of the particle densities is expressed by continuity equations. The equations are the zeroth moment of the Boltzmann equation.

$$\frac{\partial n_\alpha}{\partial t} + \nabla \cdot \left(\frac{\mathbf{j}_\alpha}{q_\alpha} \right) = \left. \frac{\partial n_\alpha}{\partial t} \right|_\Gamma \tag{2}$$

where n_α is the number density for species α and the particle fluxes are defined by the partial current densities $\mathbf{j}_\alpha = q_\alpha n_\alpha \mathbf{v}_\alpha$ in terms of the charge q_α and fluid

velocity $\mathbf{v}_\alpha$ for each species. The net production rate of species α due to atomic reactions is denoted on the right-hand side of the equation with a subscript Γ. Contributions due to atomic reactions are described later.

The first moment of the Boltzmann equation yields momentum equations for each species. The momentum equations are written in divergence form in terms of the partial current densities.

$$\frac{\partial \mathbf{j}_\alpha}{\partial t} + \nabla \cdot \left(\frac{\mathbf{j}_\alpha \mathbf{j}_\alpha}{q_\alpha n_\alpha} + \frac{q_\alpha}{m_\alpha} \mathbf{P}_\alpha \right) = \frac{q_\alpha^2 n_\alpha}{m_\alpha} \mathbf{E} + \frac{q_\alpha}{m_\alpha} \mathbf{j}_\alpha \times \mathbf{B} - \frac{q_\alpha}{m_\alpha} \sum_\beta \mathbf{R}_{\alpha\beta} + \left. \frac{\partial \mathbf{j}_\alpha}{\partial t} \right|_\Gamma \quad (3)$$

where $\mathbf{E}$ and $\mathbf{B}$ are the electric and magnetic fields, $\mathbf{P}_\alpha = p_\alpha \mathbf{I} + \mathbf{\Pi}_\alpha$ is the total pressure tensor of species α (sum of the scalar pressure and the stress tensor), and $\mathbf{R}_{\alpha\beta}$ is the momentum transfer vector from species α to species β. The net current density (momentum) generation rate of species α due to atomic reactions is denoted on the right-hand side of the equation with a subscript Γ.

The second moment of the Boltzmann equation yields energy equations for each species which are expressed in divergence form for the total energy.

$$\frac{\partial \varepsilon_\alpha}{\partial t} + \nabla \cdot \left[(\varepsilon_\alpha + p_\alpha) \frac{\mathbf{j}_\alpha}{q_\alpha n_\alpha} \right] = \mathbf{j}_\alpha \cdot \left(\mathbf{E} + \frac{\sum_\beta \mathbf{R}_{\alpha\beta}}{q_\alpha n_\alpha} \right) + \left. \frac{\partial \varepsilon_\alpha}{\partial t} \right|_\Gamma \quad (4)$$

where the total energy is defined by

$$\varepsilon_\alpha \equiv \frac{1}{\gamma - 1} p_\alpha + \frac{1}{2} m_\alpha n_\alpha v_\alpha^2 \quad (5)$$

where γ is the ratio of specific heats. An adiabatic equation of state is assumed. The energy addition rate of species α due to atomic reactions is denoted on the right-hand side of the equation with a subscript Γ and is described in a later section.

Neutral fluids can be incorporated into the multi-fluid plasma model by eliminating the species charge which returns the conventional expressions for the governing equations.

2.2.1 Electromagnetic Field Evolution

The electromagnetic fields influence the motion of the plasma fluid through the Lorentz force which is contained in Eq. (3). The motion of the plasma influences the evolution of the electromagnetic fields through the redistribution of charge density and current density. Maxwell's equations govern the evolution of the electromagnetic fields. The net charge density $\sum_\alpha q_\alpha n_\alpha$ and total current density $\sum_\alpha \mathbf{j}_\alpha$ are calculated directly from the multi-fluid equations which couple the electromagnetic fields.

$$\frac{\partial \mathbf{B}}{\partial t} = -\nabla \times \mathbf{E} \quad (6)$$

$$\epsilon_0 \mu_0 \frac{\partial \mathbf{E}}{\partial t} = \nabla \times \mathbf{B} - \mu_0 \sum_\alpha \mathbf{j}_\alpha \quad (7)$$

$$\epsilon_0 \nabla \cdot \mathbf{E} = \sum_\alpha q_\alpha n_\alpha \tag{8}$$

$$\nabla \cdot \mathbf{B} = 0 \tag{9}$$

An important area of progress is investigating accurate electromagnetic field solvers. The electromagnetic field model includes divergence constraint relations, which if not accurately satisfied, can lead to nonphysical solutions. Special treatment is required because the divergence relations over-constrain the solution. Satisfying the divergence constraint relations requires adding correction potentials to form purely hyperbolic equations [9], which requires solving additional hyperbolic equations to sweep the divergence error out of the domain or formulating Maxwell's equations with mixed potentials (scalar and vector potentials) that automatically satisfy the divergence constraint relations.

The purely hyperbolic version of Maxwell's equations are expressed as

$$\frac{\partial \mathbf{B}}{\partial t} + \nabla \times \mathbf{E} + \gamma \nabla \psi = 0 \tag{10}$$

$$\frac{\partial \mathbf{E}}{\partial t} - c^2 \nabla \times \mathbf{B} + \chi c^2 \nabla \phi = -\frac{1}{\epsilon_0} \sum_\alpha q_\alpha n_\alpha \mathbf{v}_\alpha \tag{11}$$

$$\frac{\partial \phi}{\partial t} + \chi \nabla \cdot \mathbf{E} = \frac{\chi}{\epsilon_0} \sum_\alpha q_\alpha n_\alpha \tag{12}$$

$$\frac{\partial \psi}{\partial t} + \gamma c^2 \nabla \cdot \mathbf{B} = 0 \tag{13}$$

where error propagation speeds γ and χ are introduced to convect the divergence errors out of the domain.

The electromagnetic fields can be formulated using potentials that mathematically satisfies the divergence constraint conditions, Eqs. (8) and (9). The mixed potential formulation is derived by expressing the electric and magnetic fields using scalar and vector potentials. Specifically, the scalar potential Φ and vector potential $\mathbf{A}$ are defined by

$$\mathbf{E} = -\nabla \Phi - \frac{\partial \mathbf{A}}{\partial t}, \tag{14}$$

$$\mathbf{B} = \nabla \times \mathbf{A}. \tag{15}$$

The potential formulation requires setting an arbitrary gauge condition that affects the form of the resulting governing equations. If a Coulomb gauge condition ($\nabla \cdot \mathbf{A} = 0$) is assumed, the evolution equations become

$$\nabla^2 \Phi = -\frac{1}{\epsilon_0} \sum_\alpha q_\alpha n_\alpha \tag{16}$$

$$\frac{\partial^2 \mathbf{A}}{\partial t^2} - c^2 \nabla^2 \mathbf{A} = \frac{1}{\epsilon_0} \sum_\alpha q_\alpha n_\alpha \mathbf{v}_\alpha - \nabla \left(\frac{\partial \Phi}{\partial t} \right) \tag{17}$$

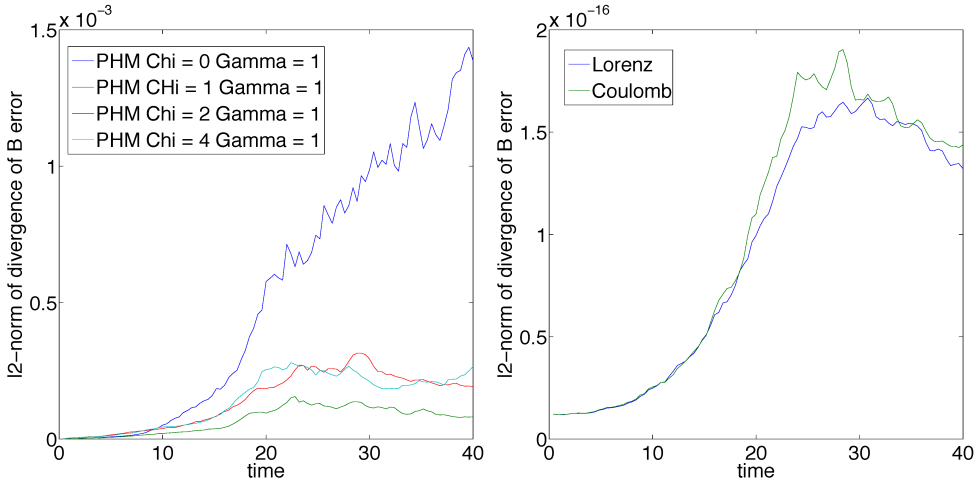

Figure 2: Evolution of the magnetic field divergence for the purely hyperbolic and mixed potential formulation of Maxwell's equations.

If the Lorenz gauge $\nabla \cdot \mathbf{A} = -\frac{1}{c^2}\frac{\partial \Phi}{\partial t}$ is assumed, the field equations become

$$\frac{\partial^2 \Phi}{\partial t^2} - c^2 \nabla^2 \Phi = \frac{c^2}{\epsilon_0} \sum_\alpha q_\alpha n_\alpha \tag{18}$$

$$\frac{\partial^2 \mathbf{A}}{\partial t^2} - c^2 \nabla^2 \mathbf{A} = \frac{1}{\epsilon_0} \sum_\alpha q_\alpha n_\alpha \mathbf{v}_\alpha. \tag{19}$$

Both the purely hyperbolic and the mixed potential formulations have been implemented to evaluate the ability of each method to preserve the divergence constraint relations. Figure 2 shows the results for the GEM challenge (Geospace Environmental Modeling Magnetic Reconnection Challenge) problem of collisionless magnetic reconnection. [24] The mixed potential formulations show a divergence error on the order of machine precision and much lower than the purely hyperbolic formulation. However, the computational effort for the mixed potential formulation is significantly greater.

2.2.2 Characteristics of the Multi-Fluid Plasma Model

As presented above, the governing equations for the multi-fluid plasma model including the electromagnetic equations are expressed in divergence form.

$$\frac{\partial Q}{\partial t} + \nabla \cdot \mathbf{F} = S \tag{20}$$

where Q is the vector of conserved fluid variables, $\mathbf{F}$ is the tensor of hyperbolic fluxes and S is the vector containing the source terms. The length of vectors depends on the number of fluids included in the model. For Q, there are

2 scalar and 1 vector variables for each fluid and 2 vector variables for the electromagnetic fields.

The system of equations can be divided into the plasma fluid equations and the electromagnetic field equations. The plasma fluid equations for species α are written as

$$\frac{\partial}{\partial t}\begin{bmatrix} n_\alpha \\ \mathbf{j}_\alpha \\ \varepsilon_\alpha \end{bmatrix} + \nabla \cdot \begin{bmatrix} \frac{\mathbf{j}_\alpha}{q_\alpha} \\ \frac{\mathbf{j}_\alpha \mathbf{j}_\alpha}{q_\alpha n_\alpha} + \frac{q_\alpha}{m_\alpha}\mathbf{P}_\alpha \\ (\varepsilon_\alpha + p_\alpha)\frac{\mathbf{j}_\alpha}{q_\alpha n_\alpha} \end{bmatrix} = \begin{bmatrix} \frac{\partial n_\alpha}{\partial t}\big|_\Gamma \\ \frac{q_\alpha^2 n_\alpha}{m_\alpha}\mathbf{E} + \frac{q_\alpha}{m_\alpha}\mathbf{j}_\alpha \times \mathbf{B} - \frac{q_\alpha}{m_\alpha}\sum_\beta \mathbf{R}_{\alpha\beta} + \frac{\partial \mathbf{j}_\alpha}{\partial t}\big|_\Gamma \\ \mathbf{j}_\alpha \cdot \left(\mathbf{E} + \frac{\sum_\beta \mathbf{R}_{\alpha\beta}}{q_\alpha n_\alpha}\right) + \frac{\partial \varepsilon_\alpha}{\partial t}\big|_\Gamma \end{bmatrix}, \quad (21)$$

The electromagnetic field equations are written as

$$\frac{\partial}{\partial t}\begin{bmatrix} \mathbf{B} \\ c^{-2}\mathbf{E} \end{bmatrix} + \nabla \times \begin{bmatrix} \mathbf{E} \\ -\mathbf{B} \end{bmatrix} = \begin{bmatrix} 0 \\ -\mu_0 \sum_\alpha \mathbf{j}_\alpha \end{bmatrix}. \quad (22)$$

Similar forms exist if either the purely hyperbolic or mixed potential formulations are used.

The Jacobians of the hyperbolic fluxes $\partial F/\partial Q$ of the governing equations [Eqs. (21) and (22)] are constructed in the usual way. The eigenvalues of the flux Jacobians give the characteristic velocities. In one dimension, the eigenvalues of the fluid equations are

$$\lambda_{fluid} = \{v_{\alpha_x}, v_{\alpha_x} \pm c_{s_\alpha}\} \quad (23)$$

where the acoustic speed for species α is defined as

$$c_{s_\alpha} = \sqrt{\frac{\gamma T_\alpha}{m_\alpha}}, \quad (24)$$

γ is the ratio of specific heats, and the temperature is defined from the scalar pressure, $p_\alpha = n_\alpha T_\alpha$.

The electron acoustic speed is larger than the ion acoustic speed for the same fluid temperatures due to the large ion to electron mass ratio. The electron acoustic speed can be larger than the Alfvén speed which is a component of the eigenvalues of MHD. The Alfvén speed for an ion/electron plasma is defined as

$$v_A = \frac{B}{\sqrt{\mu_0 \left(m_i n_i + m_e n_e\right)}} \quad (25)$$

where B is the magnetic field and μ_0 is the permeability of free space ($4\pi \times 10^{-7}$). The eigenvalues of the field equations are

$$\lambda_{field} = \{\pm c\}. \quad (26)$$

Therefore, the eigenvalues of the multi-fluid plasma model are generally not bounded by the eigenvalues of the MHD model. In general, the fastest times that must be resolved in the multi-fluid plasma model are the light transit time $\Delta x/c$ and the electron plasma oscillation time ω_{pe}^{-1}.

2.2.3 Collisional Effects

The fluids of the multi-fluid plasma model interact primarily through the electromagnetic fields which produce long-range forces. However, the short-range collisional effects can have a significant impact on the complete plasma behavior and evolution. Specifically, the collisional effects can effectively thermalize the fluids such that the complete plasma approaches a thermodynamic equilibrium.

The collisional terms allow for transfer of momentum and energy between the different fluids. [25] The terms appear as frictional effects in Eqs. (3) and (4), $\sum_\beta \mathbf{R}_{\alpha\beta}$. The rate of momentum transfer from species α to species β is given by

$$\mathbf{R}_{\alpha\beta} = m_\alpha n_\alpha \nu_{\alpha\beta} \left(\mathbf{v}_\alpha - \mathbf{v}_\beta\right). \tag{27}$$

where $\nu_{\alpha\beta}$ is the collision frequency between species α and β. Momentum conservation requires $\mathbf{R}_{\alpha\beta} = -\mathbf{R}_{\beta\alpha}$ and $\mathbf{R}_{\alpha\alpha} = 0$.

2.2.4 Atomic Reactions

The purpose of including the effect of atomic reactions into the multi-fluid plasma model is to capture the time-dependent ionization, recombination, and charge exchange reactions that are important in laboratory and transient plasmas. Atomic reactions lead to transitions between the fluids in the multi-fluid plasma model. For example, neutral ionization depletes the neutral fluid and increases the ion and electron fluids. The reactions also transfer momenta and energies between the fluids.

Contributions from atomic reactions are identified by terms on the right-hand side of Eqs. (2), (3), and (4). The terms are expressed below for the ionization (ion), recombination (rec), and charge exchange (cx) reactions for a hydrogen plasma composed of neutral hydrogen ($\alpha = n$), ionized hydrogen ($\alpha = i$), and electrons ($\alpha = e$). Additional reactions and other plasma constituents are also possible. The contributions to the species densities are

$$\left.\frac{\partial n_n}{\partial t}\right|_\Gamma = -\Gamma_{ion} + \Gamma_{rec}, \tag{28}$$

$$\left.\frac{\partial n_i}{\partial t}\right|_\Gamma = \Gamma_{ion} - \Gamma_{rec}, \tag{29}$$

$$\left.\frac{\partial n_e}{\partial t}\right|_\Gamma = \Gamma_{ion} - \Gamma_{rec}. \tag{30}$$

The contributions to the species momenta are

$$\left.\frac{m_n}{q_n}\,\frac{\partial \mathbf{j}_n}{\partial t}\right|_\Gamma = -\left(\Gamma_{ion} + \Gamma_{cx}\right) m_n \mathbf{v}_n + \left(\Gamma_{rec} + \Gamma_{cx}\right) m_i \mathbf{v}_i, \tag{31}$$

$$\left.\frac{m_i}{q_i}\,\frac{\partial \mathbf{j}_i}{\partial t}\right|_\Gamma = \left(\Gamma_{ion} + \Gamma_{cx}\right) m_i \mathbf{v}_n - \left(\Gamma_{rec} + \Gamma_{cx}\right) m_i \mathbf{v}_i, \tag{32}$$

$$\frac{m_e}{q_e}\left.\frac{\partial \mathbf{j}_e}{\partial t}\right|_{\Gamma} = \left(\Gamma_{ion} + \Gamma_{cx}\right) m_e \mathbf{v}_n - \left(\Gamma_{rec} + \Gamma_{cx}\right) m_e \mathbf{v}_e. \tag{33}$$

The contributions to the species energies are

$$\left.\frac{\partial \varepsilon_n}{\partial t}\right|_{\Gamma} = -\left(\Gamma_{ion} + \Gamma_{cx}\right) \varepsilon_n + \left(\Gamma_{rec} + \Gamma_{cx}\right) \varepsilon_i, \tag{34}$$

$$\left.\frac{\partial \varepsilon_i}{\partial t}\right|_{\Gamma} = \left(\Gamma_{ion} + \Gamma_{cx}\right) \varepsilon_n - \left(\Gamma_{rec} + \Gamma_{cx}\right) \varepsilon_i, \tag{35}$$

$$\left.\frac{\partial \varepsilon_e}{\partial t}\right|_{\Gamma} = \left(\Gamma_{ion} + \Gamma_{cx}\right) \varepsilon_n - \left(\Gamma_{rec} + \Gamma_{cx}\right) \varepsilon_e. \tag{36}$$

The reaction rates are given by

$$\begin{aligned} \Gamma_{ion} &= \langle \sigma v \rangle_{ion} n_n n_i \\ \Gamma_{rec} &= \langle \sigma v \rangle_{rec} n_e n_i \\ \Gamma_{cx} &= \langle \sigma v \rangle_{cx} n_n n_i \end{aligned} \tag{37}$$

where Γ_{ion} is the plasma source from electron impact ionization of neutrals, Γ_{rec} is the plasma sink due to recombination, and Γ_{cx} is the plasma exchange due to charge exchange. The cross sections can depend on temperature.

2.3 High-Order Discontinuous Galerkin Method

Electromagnetic forces are exerted on the plasma fluids through the source terms of Eq. (20) and the fluid motion affects the fields through the source terms of Eq. (20). Even with accurate hyperbolic flux calculations, inaccurate calculation of the source terms can lead to incorrect results. Particularly in equilibrium situations where forces from electromagnetic fields balance fluid pressure or convective forces, the contributions from the source terms must be accurately calculated to balance the divergence of the hyperbolic fluxes.

We have developed a discontinuous Galerkin method [26–28] to solve the governing equations of the multi-fluid plasma model on a computational grid. [2, 6–8] The discontinuous Galerkin method is a finite element approach that allows for arbitrarily high order basis functions to model the variation of the system variables. Source terms are automatically coupled.

The conserved variables of the multi-fluid plasma model are modeled with a set of basis functions, v_k, which can be any desired order. The governing equations, expressed as Eq. (20), are multiplied by each basis function and integrated over the mesh element volume Ω. An integral equation is generated for each basis function.

$$\int_{\Omega} v_k \frac{\partial Q}{\partial t} dV + \oint_{\partial\Omega} v_k \mathbf{F} \cdot d\mathbf{S} - \int_{\Omega} \mathbf{F} \cdot \nabla v_k dV = \int_{\Omega} v_k S dV \tag{38}$$

where the divergence theorem has been applied to the second term. The solution variables Q, flux $\mathbf{F}$, and source vector S are given by the first term, the

second term, and the right hand side of Eq. (20). The volume and surface integrals are replaced with Gaussian quadrature. The source terms are projected onto the basis functions and are, therefore, the same order accurate as the solution variables. This satisfies the high- order accuracy requirement to preserve the equilibrium balance between the divergence of the flux and the source.

The surface integral in Eq. (38) uses hyperbolic fluxes computed with a Roe-type approximate Riemann solver. [1, 29] In this method the overall solution is built upon the solutions to the Riemann problem defined by the discontinuous jump in the solution at each element interface. The numerical flux for a first-order accurate (in space) Roe-type solver is written in symmetric form as

$$F_{i+1/2} = \frac{1}{2}\left(F_{i+1} + F_i\right) - \frac{1}{2}\sum_k l_k \left(Q_{i+1} - Q_i\right) |\lambda_k| \, r_k \tag{39}$$

where r_k is the k^{th} right eigenvector, λ_k is the k^{th} eigenvalue, and l_k is the k^{th} left eigenvector, evaluated at the element interface $(i + 1/2)$. The values at the element interface are obtained by a Roe average of the neighboring elements. The flux calculated as above is normal to the element interface which is the desired orientation for calculating the surface integral.

For the two-dimensional, second-order accurate algorithm, a linear set of basis functions are used.

$$\{v_k\} = \{v_0, v_x, v_y\} = \left\{1, \frac{x - x_{ij}}{\Delta x/2}, \frac{y - y_{ij}}{\Delta y/2}\right\} \tag{40}$$

where the center of the mesh element is located at (x_{ij}, y_{ij}) and extends Δx by Δy. The conserved variables Q are defined as

$$Q = Q_0 + Q_x v_x + Q_y v_y \tag{41}$$

within each mesh element. Update equations for the coefficients for each conserved variable are found directly from Eq. (38) applied to each mesh element.

The temporal evolution is determined with a Runge-Kutta method. A third order TVD method has been used successfully.

Extensions to higher order involves increasing the order of the basis functions and following the evolution of the additional coefficients. For example the third-order accurate basis functions would have the form

$$\{v_k\} = \{v_0, v_x, v_y, v_{xy}, v_{xx}, v_{yy}\}. \tag{42}$$

and each conserved variable Q is defined as

$$Q = Q_0 + Q_x v_x + Q_y v_y + Q_{xy} v_{xy} + Q_{xx} v_{xx} + Q_{yy} v_{yy} \tag{43}$$

within each mesh element.

The discontinuous Galerkin algorithm has been applied to the electromagnetic plasma shock demonstrating the transition from gas dynamic shocks to the MHD shock [30, 31] as the Larmor radius is reduced. Analysis of the data

shows the differences caused by the additional plasma waves that are captured in the two-fluid model and, consequently, in the algorithm developed here. [1] It also illustrates the dispersive nature of the waves which makes capturing the effect difficult in MHD algorithms. The electromagnetic plasma shock serves to validate the algorithm to published data (MHD limit) and analytical results (gas dynamic limit). The algorithm has also been applied to study collisionless reconnection and the results are compared to published results of the GEM challenge problem. [24] The problem is difficult to model and provides a rigorous test for the algorithm and benchmarks to other algorithms. The evolution of the reconnected magnetic flux compares remarkably well with the published data. [2] Additional applications are discussed in more detail below.

2.4 Time-Integration Methods

The Runge-Kutta method described previously has proven to be robust and accurate for explicit calculations. The multi-fluid plasma model has disparate characteristic speeds and frequencies. The speeds range from the high speed of light and electron plasma frequency (nanosecond times) to slow speed of bulk fluid motion or ion sound speed (second or longer times). The short time scales dictate a small time-step for any explicit time-integration method. Using the high-order discontinuous Galerkin method further exacerbates the small time-step.

The fast time scales contained in the multi-fluid plasma model are identified by the eigenvalues discussed in Sec. 2.2. When phenomena of interest occurs on these time scales then time steps of this size must be used. When phenomena of interest occurs on longer time scales then it is desirable to use appropriately large time steps. As discussed earlier, asymptotic approximations can be applied to the multi-fluid plasma model to remove the most severe time scale constraints; however, these approximations fundamentally change the physical model and yield an equation system that can be more difficult to solve mathematically. We propose to instead investigate mathematical methods that allow time steps larger than the fastest time scales.

Fully implicit methods have been investigated. The governing equations are written as

$$\frac{\partial Q}{\partial t} = f(Q). \tag{44}$$

The time advance can be expressed in an implicit form of arbitrary order accuracy as

$$Q^{n+1} = g\left(\Delta t, Q^{n+1}, Q^n, Q^{n-1}, ...\right). \tag{45}$$

A second-order Crank-Nicolson method has been implemented, where the time advance equation is written as

$$Q^{n+1} = Q^n + \frac{\Delta t}{2}\left[f\left(Q^{n+1}\right) + f\left(Q^n\right)\right], \tag{46}$$

which is solved iteratively using a variety of implicit numerical methods, e.g. Conjugate Residual, Biconjugate Gradient, and GMRES, with preconditioners

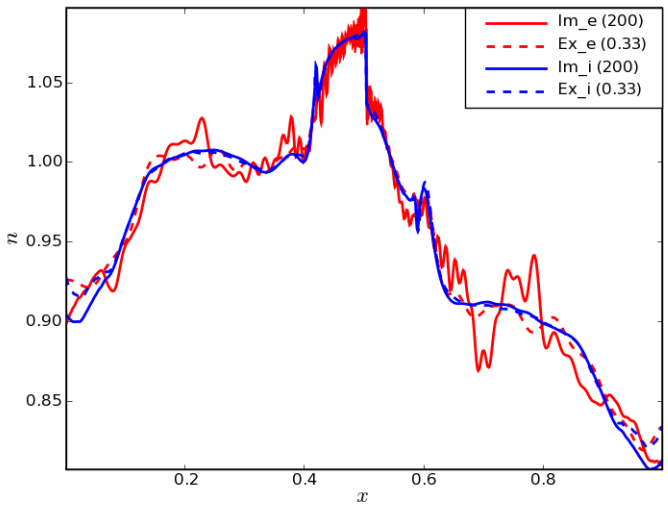

Figure 3: Electron and ion number densities for the electromagnetic shock problem solved with the implicit method using time steps 200 times larger than the fastest time system time scale. An explicit solution is also shown for comparison.

such as Incomplete LU and Additive Schwarz. The method has been applied to several benchmark problems to compare the accuracy of the solution when large time steps are used. Solution accuracy is well preserved for the resolved timescale. However, the full implicit time integration is inefficient because of the large size of the equation system.

The electromagnetic shock problem provides a rigorous benchmark because it has fast phenomena associated with light and whistler wave propagation, and it has slower phenomena associated with the massive ion motion. Figure 3 shows simulation results for the ion and electron number densities for the electromagnetic shock problem where steps 200 times larger than the light transit time and 20 times larger than the electron characteristic time are used. An explicit solution which resolves all of the time scales is also shown for comparison. The solution shows that the electron dynamics are only approximately modeled by the implicit method as expected, but the ion dynamics are well captured and agree with the explicit solution. Both methods use a second-order discontinuous Galerkin spatial representation.

A semi-implicit method has been formulated to perform a splitting of the governing equations of the two-fluid plasma model. The splitting is based on the different expected physics and corresponding different scales dictated by the specific model equations. Specifically, the electron fluid and electromagnetic fields introduce the fast/small scales and are solved implicitly using the method described by Eq. (46), and the ions introduce slow/large scales and

are solved explicitly using the third-order accurate TVD Runge-Kutta time advance method. The combination of implicit and explicit treatments limits the size of the operator matrix while still allowing time steps that are not limited by the fast timescales. The time step is still limited by the ion motion; however, the ion motion is often the timescale of interest and needs to be resolved for accurate simulation results. The semi-implicit method has yielded encouraging results by exploiting the fundamental physics of the governing equations. However, there are additional avenues to pursue to further incorporate the physics of the governing equations into the numerical method.

2.5 Applications

The described above is implemented on parallel computers using an automatic domain decomposition technique with MPI message passing. The algorithm is implemented in a code called WARPX (Washington Approximate Riemann Plasma) which uses C++ object oriented programming and other modern software techniques to simplify the maintainability and extendibility of the code and HDF5 for parallel output.

2.5.1 Field Reversed Configurations (FRC) in Three Dimensions

WARPX has been applied to study Z-pinch dynamics and three-dimensional FRC evolution to investigate anomalous resistivity that experimentally limits the plasma current. An experiment at Kirtland AFB (AFRL/RDHP) forms FRC plasmas, translates them into a cylindrical flux conserver, and compresses the plasma to high energy densities by imploding the flux conserver onto the plasma. FRC plasmas have been modeled using MHD codes with unsatisfactory results. Specifically, FRC plasmas are characterized by large gyroradii ($L/r_L = 2 - 4$) and charge separation. MHD models have failed to predict many experimental observations, such as observed stability and anomalous resistivity. The lack of agreement is conjectured to be caused by two-fluid effects. Sample evolutions of the FRC plasmoid are shown in Fig. 4.

2.5.2 Three-Fluid Plasma Model for Plasma Production

WARPX provides a flexible code framework that allows easy extension of the physical model to include multiple fluids. We have extended WARPX to a three-fluid (electrons, ions, and neutrals) simulation of plasma sheath formation. Atomic reactions are incorporated that describe the effects of collisions between the species explicitly, allowing for the identification of regions of ionization/recombination and interspecies momentum and energy transfer. Plasma sheath formation is important for electrode-based plasma technologies, e.g. plasma actuators for control of high-speed aerospace vehicles. The multi-fluid model captures electron inertial effects and has revealed a new physical effect.

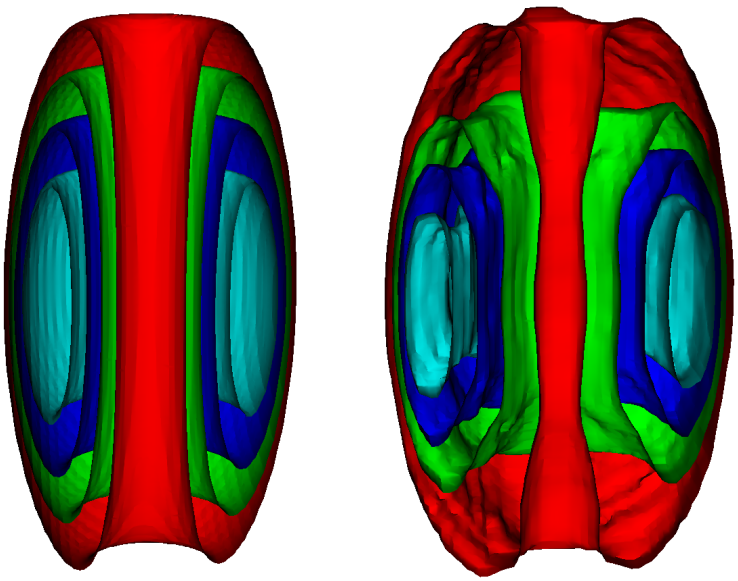

Figure 4: Three-dimensional evolution of an FRC using the WARPX code. Small scale variations are evident in the azimuthal direction indicative of a drift instability.

During the initial formation of the plasma sheath the applied electrode potential excites a Langmuir wave that propagates into the bulk plasma. The dispersion relation is given by

$$\omega^2 = \omega_{pe}^2 + \frac{3}{2}k^2 v_{Te}^2. \tag{47}$$

Typically, sheath simulations assume electrostatic fields and miss the electrodynamics of the formation process. Propagating Langmuir waves are shown in simulation results in Fig. 5. The numerical dispersion agrees with the dispersion relation of Eq. (47).

The plasma sheath formation studies provide better physical understanding into the plasma production process. Plasma (ions and electrons) is produced by ionizing the neutral gas, and it is lost when it reaches the electrode and recombines. An analytical model of the electrode describes secondary electron emission and recombination at the electrode. In addition to the plasma sheath that naturally forms around electrodes, a voltage can be applied to the electrodes to drive a current through the plasma. Phenomena such as cathode and anode drops are accurately simulated.

3 Conclusions

Investigating advanced plasma models is motivated by the need to simulate complicated plasma physics phenomena that is not captured in simpler models.

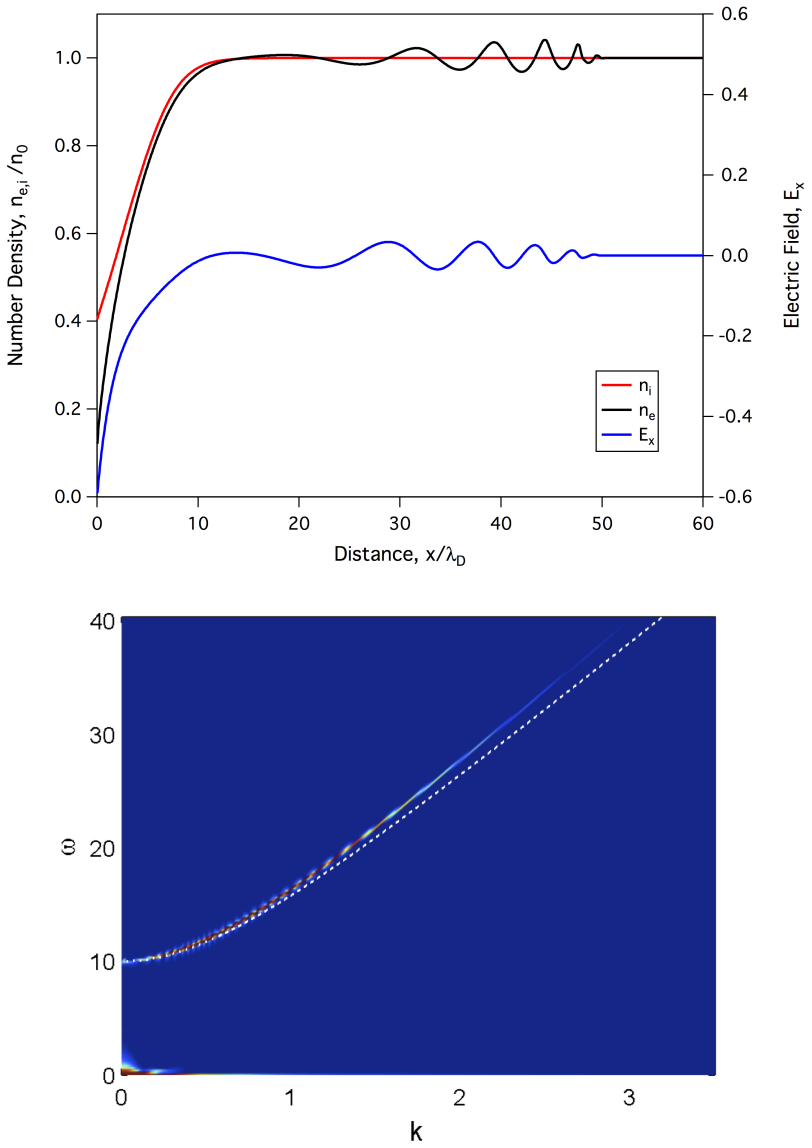

Figure 5: Initial plasma production showing the propagation of a Langmuir wave in the electron density (black trace) and electric field. Numerical dispersion calculated in (k,ω) space agrees with analytical dispersion relation (dashed line).

The multi-fluid plasma model is proving to be a model that is significantly more advanced and complete than the usual MHD model without the computational complexity required in general kinetic models. This project has developed the multi-fluid plasma model and cast the governing equations in a balance law form that lends itself to accurate numerical solutions. The algorithm developed in the project, its implementation into WARPX, and its application to benchmark and real experimental problems have demonstrated the capability of both the multi-fluid plasma model and the numerical techniques in the algorithm.

Acknowledgment/Disclaimer

This work was sponsored by the Air Force Office of Scientific Research, USAF, under grant number FA9550-09-1-0135. The views and conclusions contained herein are those of the author and should not be interpreted as necessarily representing the official policies or endorsements, either expressed or implied, of the Air Force Office of Scientific Research or the U. S. Government.

References

[1] U. Shumlak and J. Loverich. Approximate Riemann solver for the two-fluid plasma model. *Journal of Computational Physics*, 187(2):620 – 638, 2003.

[2] J. Loverich and U. Shumlak. A discontinuous Galerkin method for the full two-fluid plasma model. *Computer Physics Communications*, 169(1-3):251 – 255, 2005.

[3] A. Hakim, J. Loverich, and U. Shumlak. A high resolution wave propagation scheme for ideal two-fluid plasma equations. *Journal of Computational Physics*, 219(1):418 – 442, 2006.

[4] J. Loverich and U. Shumlak. Nonlinear full two-fluid study of $m = 0$ sausage instabilities in an axisymmetric Z pinch. *Physics of Plasmas*, 13(8):082310, 2006.

[5] A. Hakim and U. Shumlak. Two-fluid physics and field-reversed configurations. *Physics of Plasmas*, 14(5):055911, 2007.

[6] J. Loverich, A. Hakim, and U. Shumlak. A discontinuous Galerkin method for ideal two-fluid plasma equations. *Communications in Computational Physics*, 9:240–268, 2011.

[7] B. Srinivasan, A. Hakim, and U. Shumlak. Numerical methods for two-fluid dispersive fast MHD phenomena. *Communications in Computational Physics*, 10:183–215, Mar 2011.

[8] U. Shumlak, R. Lilly, N. Reddell, E. Sousa, and B. Srinivasan. Advanced physics calculations using a multi-fluid plasma model. *Computer Physics*

Communications, 182(9):1767 – 1770, 2011. Computer Physics Communications Special Edition for Conference on Computational Physics Trondheim, Norway, June 23-26, 2010.

[9] C. D. Munz, P. Ommes, and R. Schneider. A three-dimensional finite volume solver for the Maxwell equations with divergence cleaning on unstructured meshes. *Computer Physics Communications*, 130:83–117, 2000.

[10] A. R. Bell. Computational Simulation of Plasmas. *Astrophysics and Space Science*, 256:13–35, 1998.

[11] CZ Cheng and G Knorr. Integration Of Vlasov Equation In Configuration Space. *Journal of Computational Physics*, 22(3):330–351, 1976.

[12] H Ruhl and P Mulser. Relativistic Vlasov Simulation Of Intense Fs Laser Pulse-Matter Interaction. *Physics Letters A*, 205(5-6):388–392, Sep 1995.

[13] L Chacon, DC Barnes, DA Knoll, and GH Miley. An implicit energy-conservative 2D Fokker-Planck algorithm. *Journal of Computational Physics*, 157(2):618–653, 2000.

[14] L Chacon, DC Barnes, DA Knoll, and GH Miley. An implicit energy-conservative 2D Fokker-Planck algorithm - II. Jacobian-free Newton-Krylov solver. *Journal of Computational Physics*, 157(2):654–682, 2000.

[15] C. K. Birdsall and A. B. Langdon. *Plasma Physics via Computer Simulation*. McGraw-Hill, New York, 1985.

[16] J. P. Freidberg. Ideal magnetohydrodynamic theory of magnetic fusion systems. *Reviews of Modern Physics*, 54(3):801–902, July 1982.

[17] R. E. Peterkin Jr., M. H. Frese, and C. R. Sovinec. Transport of Magnetic Flux in an Arbitrary Coordinate ALE Code. *Journal of Computational Physics*, 140(1):148–171, Feb 1998.

[18] U. Shumlak, T. W. Hussey, and R. E. Peterkin Jr. Three-Dimensional Magnetic Field Enhancement in a Liner Implosion System. *IEEE Transactions on Plasma Science*, 23(1):83–88, Feb 1995.

[19] O. S. Jones, U. Shumlak, and D. S. Eberhardt. An implicit scheme for nonideal magnetohydrodynamics. *Journal of Computational Physics*, 130(2):231 – 242, 1997.

[20] B. Udrea and U. Shumlak. Nonlinear study of spheromak tilt instability. In *AIAA 36th Aerospace Sciences Meeting & Exhibit*, Reno, Nevada, January 1998. AIAA Paper No. 98-0995.

[21] R. E. Peterkin and P. J. Turchi. Magnetohydrodynamic theory for hypersonic plasma flow - what's important and what's not. In *AIAA 31st Plasmadynamics and Lasers Conference*, Denver, Colorado, June 2000. AIAA Paper No. 2000-2257.

[22] D. Harned and Z. Mikic. *Journal of Computational Physics*, 83:1, 1989.

[23] J. T. Becerra Sagredo. Semi-implicit treatment of the hall term in finite volume, mhd computations. Master's thesis, University of Washington, Seattle, WA 98195, June 1998.

[24] J. Birn, J. F. Drake, M. A. Shay, B. N. Rogers, R. E. Denton, M. Hesse, M. Kuznetsova, Z. W. Ma, A. Bhattacharjee, A. Otto, and P. L. Pritchett. Geospace Environmental Modeling (GEM) Magnetic Reconnection Challenge. *Journal of Geophysical Research*, 106(2):3715, 2001.

[25] S. I. Braginskii. Transport processes in a plasma. In M. A. Leontovich, editor, *Reviews of Plasma Physics*, volume 1, pages 205–311. Consultants Bureau, New York, NY, 1965.

[26] B Cockburn and CW Shu. TVB Runge-Kutta Local Projection Discontinuous Galerkin Finite-Element Method For Conservation-Laws. *Mathematics Of Computation*, 52(186):411–435, 1989.

[27] B Cockburn, SC Hou, and CW Shu. The Runge-Kutta Local Projection Discontinuous Galerkin Finite-Element Method For Conservation-Laws. *Mathematics Of Computation*, 54(190):545–581, 1990.

[28] B Cockburn and CW Shu. The Runge-Kutta discontinuous Galerkin method for conservation laws. *Journal of Computational Physics*, 141(2):199–224, 1998.

[29] P. L. Roe. Approximate riemann solvers, parameter vectors and difference schemes. *Journal of Computational Physics*, 43:357, 1981.

[30] M. Brio and C. C. Wu. *Journal of Computational Physics*, 75:400, 1988.

[31] A. L. Zachery and P. Colella. *Journal of Computational Physics*, 99:341, 1992.